Mühendis ve Makina
cilt 63, sayı 709, s. 616-632, 2022
Araştırma Makalesi

Engineer and Machinery
vol. 63, no. 709, p. 616-632, 2022
Research Article

DOI : 10.46399/muhendismakina.1109325

Performance Modelling of Landing Gear and Suspension System of a Flying Car for Landing and Bump Passing Manoeuvres

Murat Ötkür[*1], Ali Dinç[2]

ABSTRACT

Recent research and development activities in both in aviation and automotive industries resulted with a genuine product known as roadable aircraft also known as flying car. Roadable aircraft is combination of a small size airplane and a passenger vehicle containing the superior sides of both products; and provides door-to-door transportation by both ground and air. Many companies invested in this product and first commercial units are expected to be the launched within 5 years.

Suspension system of a roadable aircrafts plays a significant role in the overall product design, as it should satisfy the customer requirements for both aircrafts and passenger cars: landing and traveling on road. In this study, suspension system of a flying car was modelled in Matlab/Simulink and optimized as a quarter car model employing a 2 DOF Mass-Spring-Damper system. The equations of motion were presented, and the model was firstly simulated as an aircraft landing gear for landing performance. Then the model was run to determine driving performance on road for a typical bump passing manoeuvre. A set of design parameters was determined for acceptable performance outputs: suspension system damping element acting force and displacement for the landing and maximum acceleration for the bump passing performance.

Keywords: Aircraft landing gear, flying car/roadable aircraft, shock absorber

Uçan Arabaların İniş Takımı ve Süspansiyon Sisteminin, İniş ve Engel Geçme Manevraları için Performans Modellemesi

ÖZ

Havacılık ve otomotiv sektöründeki son zamanlarda yapılan araştırma ve geliştirme çalışmaları neticesinde uçan araba geliştirilmiştir. Uçan arabalar küçük bir uçak ve binek araç taşıtlarının birleştirilmesinde oluşup, her iki taşıdın da üstün özelliklerini taşımaktadırlar ve hem kara ve hem hava yolu taşımacılığı için kapıdan kapıya ulaşım sağlamaktadırlar. Ticari olarak birçok firma son zamanlarda uçan arabalara yatırım yapmakta olup, 5 yıl içerisinde nihai müşteriye ürün satışı beklenmektedir.

Uçan araçların süspansiyon sistemi tasarımı, bu sistemlerin hem uçak hem de binek araç müşterilerinin gereksinimlerini karşılaması gerektiği için; ürün geliştirme sürecinde oldukça önemli bir yer kaplamaktadır. Bu çalışmada bir uçan arabanın süspansiyon sistemi, 2 serbestlik dereceli Kütle-Yay-Sönümleyici sistemi kullanılarak çeyrek araç modeli prensiplerine göre Matlab/Simulink programında modellenmiştir. İlgili hakaret denklemler verilip, model iniş takımları için öncelikle bir iniş manevrası simülasyonu için çalıştırılmıştır. Sonrasında aynı model araç sürüş simülasyonu doğrultusunda engel geçme manevrası için kullanılmıştır. Çalışma neticesinde uçan araba tasarımı tasarım parametreleri için kabul edilebilir performans parametreleri kümesi tanımlanmıştır: süspansiyon sistemi sönümleme elemanı üzerindeki kuvvet, iniş manevrası süspansiyon sistemi yer değiştirmesi ve engel geçme manevrasındaki maksimum ivme.

Anahtar Kelimeler: Uçak iniş takımları, uçan araba, süspansiyon sistemi

[*] İletişim Yazarı

Geliş/Received : 26.04.2022
Kabul/Accepted : 29.08.2022

[1] College of Engineering and Technology, American University of the Middle East, Kuwait, Engineering and Technology, Mechanical Engineering Department, Egaila, Murat.Otkur@Aum.Edu.Kw, ORCID: 0000-0002-6160-4188

[2] College of Engineering and Technology, American University of the Middle East, Kuwait, Engineering and Technology, Mechanical Engineering Department, Egaila, Ali.Dinc@Aum.Edu.Kw, ORCID: 0000-0002-3165-3421

1. INTRODUCTION

Transportation industry is mainly dependent on road transportation for centuries and the highest percentage of the vehicle type is passenger car. The number of registered passenger cars in the world is more than 1 billion. The number is increased by 25%, if the commercial vehicles are added as well. The high number of vehicles, comes with the traffic congestion problem especially in the crowed cities like İstanbul, New York, London, Shanghai, etc. In order to overcome the traffic congestion problem, inventors came with the idea of flying cars. Flying cars are considered as hybrid vehicles, that acts like a car on road and like a small plane in the air. They should satisfy the requirements of both vehicle types. The suspension system of the flying car has the regular function of a road vehicle while driving on the road and performs the functions of a landing gear of the plane during the landing manoeuvre. Therefore, design and optimization of the suspension system should consider the requirements for both cases. Consequently, the research question is to develop a methodology for defining the suspension system parameters that will fulfil the requirements of both comfort driving on road and landing manoeuvres. Withing this perspective, the suspension system of a flying car is mathematically modelled and virtually tested for bump passing manoeuvre on road in order to assess the comfort requirements and for a landing manoeuvre as well. The paper is structed with literature review related with flying cars in section 2, the methodology in section 3, the results of the study in section 4, the discussion about the results in section 5 and the conclusion in section 6.

2. LITERATURE REVIEW

Roadable aircrafts have been in the interest of researcher and entrepreneurs for almost a century. There have been numerous studies in literature regarding roadable aircraft or flying car designs which may provide several benefits for traffic congestion, mobility, fast and easy transport etc. The first roadable aircraft design was developed by Glenn Curtiss in 1917, and although the plane was capable of lifting off the ground, it never achieved full flight [1]. Between 1925 and early 1990s, 19 roadable aircraft projects have been studied with a distribution rate of 3 concepts, 3 prototypes and 13 flying prototypes [2]. Unfortunately, none of them turned into commercial products due to the safety and feasibility issues.

In the last 3 decades, most of the studies remained at conceptual level mainly focusing on aerodynamics, structural mechanics, materials, functionality, configuration and suspension system etc. Stiles presented a new roadable aircraft concept that combines canard aircraft and passenger car with engine located at the centre [1]. The main wings have the ability to rotate around pivot point. Kettering and Biezad studied a roadable aircraft project with a preliminary design that was intended to be used as a mobile aero systems test laboratory in the undergraduate aeronautical engineering

curriculum at California Polytechnic State University [3]. Follmann and Cunha examined a triphibian flying car design, that has the capability of fly, drive and sail for door-to-door transportation using any media [4]. Crow designed a practical flying vehicle with three wheels and detachable wings that are attached to the fuselage at sky mode and removed on road mode [5]. The vehicle had a gross weight of 1180 lbs including the wings and powered with a single engine. Sarh and Clausen studied private air transportation with time saving considering inter-city and intra-city distances for a roadable aircraft, named as "Advanced Flying Automobile (AFA)", and compares with automobiles for chosen distances through assessing the value of travel time and expenses per vehicle and mile [6]. Ott studied a conceptual design of a vertical take-off and landing (VTOL) flying car named HELIos - a single seat and three-wheel car – using duct enclosed counter-rotating propellers eliminating the need for a tail rotor [7]. Nakajima et al. studied a roadable aircraft design with fixed circular wing at the top of the vehicle and the investigation of the aerodynamic characteristics [8]. They evolved the circular design to a D-style wing design and performed wind tunnel tests on a small-scale wing prototype studying the structural analysis and drag coefficient effects [9]. Murai and Hayashi (2006) worked on a conceptual roadable aircraft with an inflatable wing design and performed the finite element analysis using MARC software [10]. Additionally, they studied a concept of a roadable landing gear which is expected to satisfy road driving customer requirements. Haskins et al. studied the pulsed turbine rotor engine VTOL propulsion concept and applications: capturing the elusive jet-powered flying car and redesigning a radical variant of the V-22 Osprey [11]. Saeed and Gratton made an evaluation of the historical issues associated with achieving non-helicopter vertical and short take-off and landing (V/STOL) capability and the search for the flying car concept [12]. Giannini et al. performed a conceptual design of a VTOL roadable aircraft that was preceded by an exhaustive literature study including critical technologies such as hybrid electric drive, advanced batteries, variable geometry, ducted fan propulsion systems, advanced lightweight heavy fuel engines, lightweight materials, advanced sensors, and flight controls for stable transition from vertical to horizontal flight [13]. Over the last few years, significant developments in automotive and aviation industries have shown that flying cars are expected to be introduced in the automotive and aviation market between 2020 and 2025 with valuable contributions of various start-ups such as Terrafugia, AeroMobil and well-established automobile and aviation manufacturing companies such as Airbus, Audi, Rolls Royce, Aston Martin, etc… [14].

A flying car can be considered as a synthesis of a small aircraft and passenger vehicle and various systems of the car should satisfy the customer requirements related engineering specifications of both aircrafts and the road vehicles such as suspension system. It works not only during the landing manoeuvre of the aircraft with the objective of minimizing the impact forces and but also during road driving in order to pro-

vide a comfortable ride for the passengers and reduce the impact forces on the body components. Suspension systems work using the principle of isolating the vehicle body from the road by means of spring and damper components. Depending on these components constants, suspension system can be categorized in three types: passive, semi-active and active. In passive suspension, both spring and damper coefficients are constants, whereas in semi-active type, the damper coefficient can be adjusted depending on operating conditions. In active suspension systems, an additional actuator is used with the output of displacement or force. There have been numerous studies about suspension system modelling and analysis, investigating system response in passive, semi-active and active suspension systems. Independent of the suspension system type the ultimate goal for road driving conditions is to generate a comfortable ride for the passenger. Ahlin and Granlund established a model for predicting vertical human whole body vibrations in a typical passenger car, using data from any measured road roughness profile that can be used as part of the foundation of road roughness management policies in order to determine the reference ride quality using ISO 2631 vibration evaluation [15]. Konieczny worked on analysis of simplifications applied in vibration damping modelling for a passive hydraulic car shock absorber modelled using a two degree of freedom (2-DOF) [16]. Darsivan and Faris investigated the response and accuracy of a 2-DOF quarter car model with nonlinear shock absorber damping force with parameters inherited from a previously verified experiment [17]. Luczko and Ferdek studied non-linear analysis of a 2-DOF quarter car model with stroke-dependent twin-tube shock absorber containing an additional double-chamber cylinder providing the advantage of protecting shock absorber against damage in the case of large amplitudes of excitations and maintaining driving comfort with soft characteristics of small amplitude high frequency excitations [18]. Active control of damping provides better comfort characteristics. Jahromi and Zabihollah introduced a novel semi-active control system for suspension systems of passenger car using Magneto Rheological (MR) dampers on 8-DOF full car model [19]. Each suspension system consisted of a passive and active damper. The control mechanism is designed based on the optimal control algorithm, Linear Quadratic Regulator (LQR). Aggarwal investigated vibration control performance of a 3-DOF quarter car model with MR shock absorber suspension system using forward fuzzy logic controller (FFLC) and inverse fuzzy logic controller (IFFL) [20]. Simulation results were compared for selection of best controller that can provide maximum ride comfort to travelling passengers and safety.

Aircraft landing gear design experience can be used for flying cars. Flugge studied landing gear impact force for landing and taxying manoeuvres excluding drag forces [21]. Similarly, Milwitzky and Cook presented a theoretical study of the conventional type of oleo pneumatic landing gear behaviour at NASA [22]. Conway wrote a good book on landing gear design [23]. Currey explained aircraft landing gear design prin-

ciples and practices [24]. Karam and Mare advanced model development and validation of landing gear shock struts [25]. Pratomo et al. worked on the design and analysis of upper wishbone for suspension system on vertical take-off and landing (VTOL) propulsion system flying car [26].

3. METHODOLOGY

An aircraft landing gear can be modelled as 2-DOF mass-spring-damper system similar to a quarter car model considering during the landing manoeuvre of the aircraft, contact between the aircraft and ground is realized only on the landing gear wheels. Figure 1 shows a simplified model of landing gear. In this model the shock absorber was modelled as a spring (with coefficient k_1) and a damper (with coefficient b), tire was modelled as a spring (with coefficient k_2). Mass of aircraft was modelled as a portion per landing gear (m_1) and mass of the landing gear and the tire is directly added to the model as the second mass (m_2). Acceleration of both masses in the vertical direction are calculated based on Newton's second law as shown in differential equations 1 & 2. Equation 1 is for the aircraft mass and equation 2 is for the landing gear and tire mass. Initial vertical velocities of both of the masses are set as the sink/landing vertical speed of the aircraft and initial positions are set as 0 and updated afterwards with respect to initial position.

$$m_1 \ddot{x}_1 = \mathrm{M} - \mathrm{L} - b\left(\dot{x}_1 - \dot{x}_2\right) - k_1\left(x_1 - x_2\right) \tag{1}$$

$$m_2 \ddot{x}_2 = b\left(\dot{x}_1 - \dot{x}_2\right) + k_1\left(x_1 - x_2\right) - k_2\left(x_2 + w\right) \tag{2}$$

where k_1 & k_2 represent the spring stiffness coefficient of the landing gear and the tire, b represents the shock absorber damping coefficient of the landing gear, x_1 & x_2 represent the displacements of the masses m_1 & m_2, $\dot{x}_1$ &$\dot{x}_2$ represent the velocities of the masses m_1 & m_2, $\ddot{x}_1$ &$\ddot{x}_2$ represent the accelerations of the masses m_1 & m_2, W represents the position of the ground for the taxi manoeuvres, and L and M represent the lift force and weight of the aircraft per landing gear.

Equations 1 & 2 are applicable for both landing and taxing manoeuvres. For the landing manoeuvre the position of the ground W is considered as 0 and for the taxing manoeuvre, it is defined with respect to the bumper profile. The mathematical block diagram model was constructed in Matlab/Simulink based on equations 1 & 2, as shown in Figure 2. Landing gear suspension is assumed to be consisting of air spring and oil damper. Air spring stiffness coefficient is depicted in Figure 3-a. There is a nonlinear behaviour of the spring force increasing exponentially due to compression of the air. Similarly, oil orifice area is shown in Figure 3-b. Additional parameters used in the suspension system is listed at Table 1. Model is validated for the landing mano-

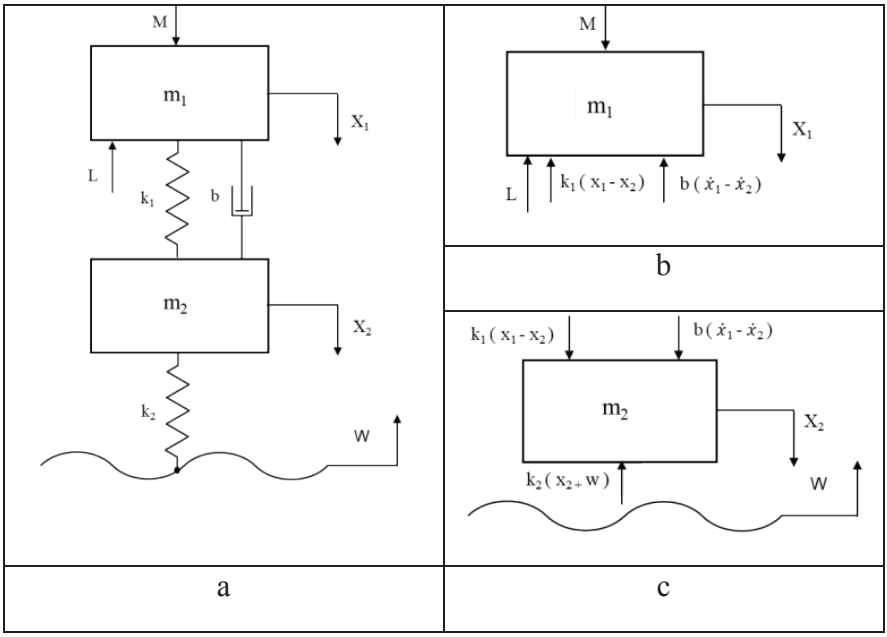

Figure 1. Quarter Car Suspension Model (a) and FBDs (b & c) for Landing Gear

Table 1. Suspension System and Aircraft Parameters For Landing Gear Validation Model

Parameter	Unit	Value
Hydraulic Area of Shock Strut	m^2	0.0256774
Oil Density	kg/m^3	870
Discharge Coefficient of Damper	-	1
Tyre Spring Coefficient	kN/m	2953
Aircraft Mass Per Landing Gear	kg	18103
Mass of Tyre	kg	59.4
Vertical Sink Speed	m/s	3.048

euvre using data inherited from landing gear impact report by W. Flügge "Technical Note 2743" as depicted in Figure 4.

Table 1. Suspension system and aircraft parameters for landing gear validation model.

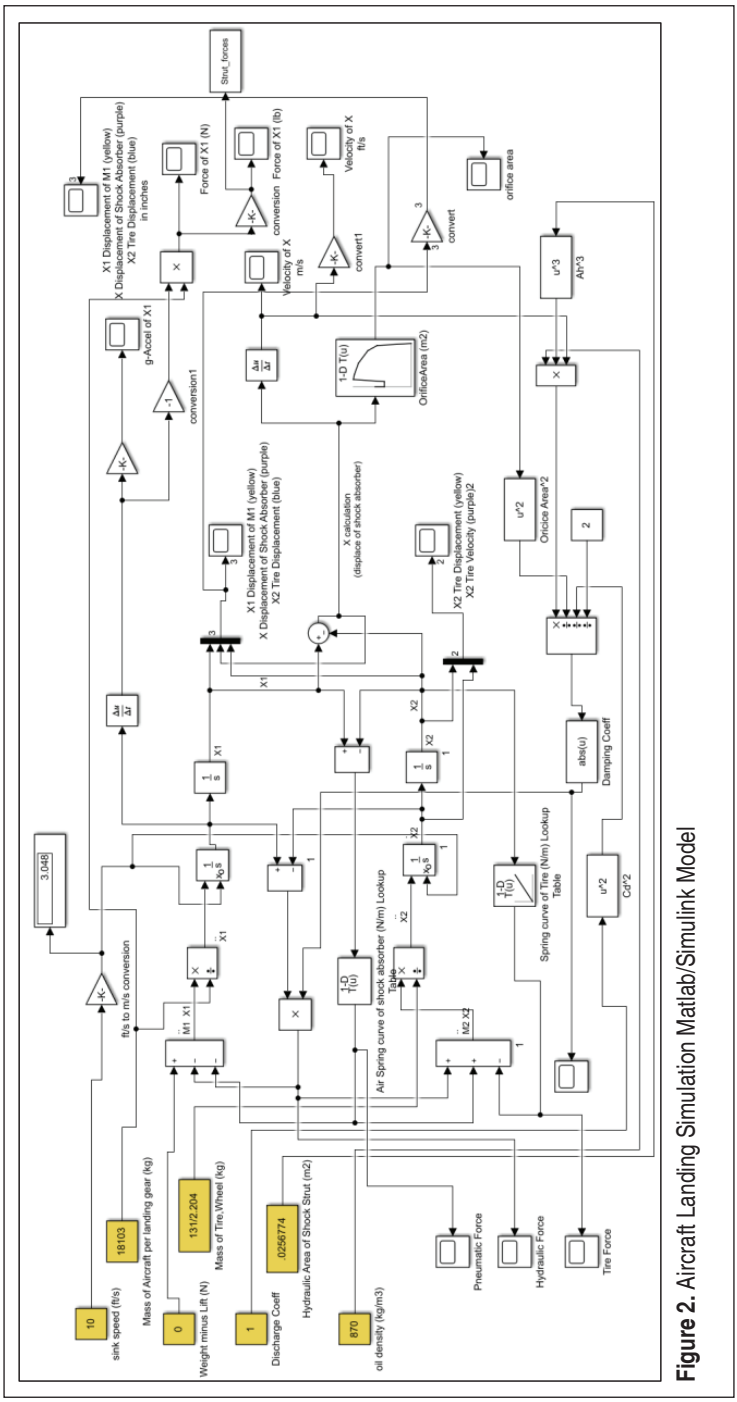

Figure 2. Aircraft Landing Simulation Matlab/Simulink Model

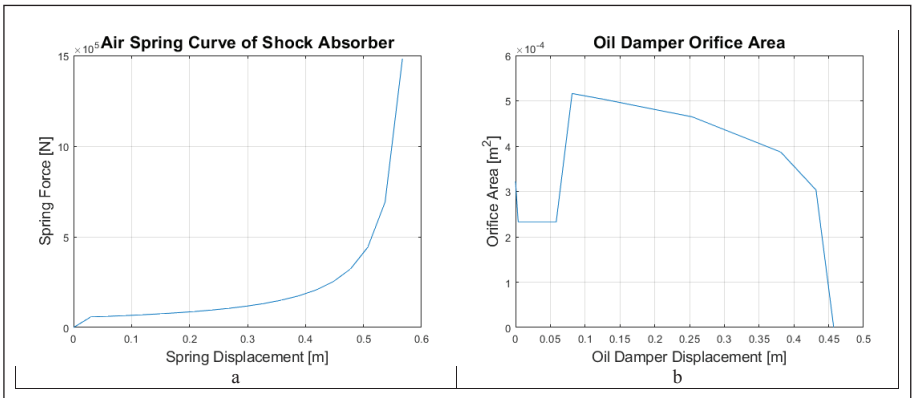

Figure 3. Landing Gear Air Spring Stiffness Coefficient (a), Landing Gear Oil Damper Orifice Area (b)

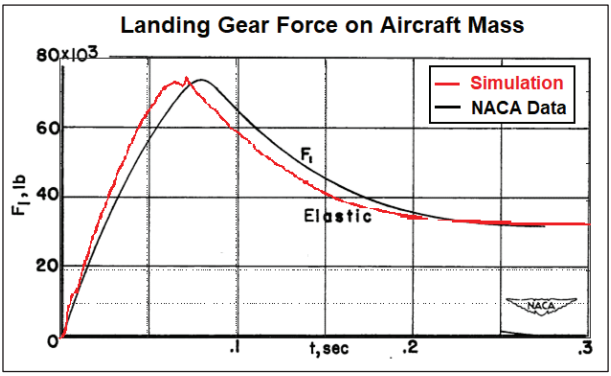

Figure 4. Landing Gear Force on Aircraft Mass Comparison: NACA Data and Simulation

Flying cars' suspension system should be designed considering landing and taxing manoeuvres. Therefore, a new Matlab/Simulink model is generated that is capable of simulating landing and taxing manoeuvres as shown on Figure 6. Switching between the manoeuvres is realized using manual switch blocks.

Two scenarios are investigated for the flying car with the developed model: landing and bump passing. Input parameters of the model for the landing and bump passing scenarios are summarized in Table 2. Considering the landing manoeuvre, only the suspension system at the rear axle of the flying car is considered. As the suspension

Table 2. Matlab/Simulink Model Parameters for Flying Car

Parameter	Unit	Value
Flying car mass	kg	1500
Flying car mass per landing gear	kg	750
Wing lift / Aircraft weight ratio	-	2/3
Mass of the landing gear and tire	kg	59.4
Landing gear damping coefficient	Ns/m	5000
Landing gear spring stiffness coefficient	N/m	60000
Tire spring stiffness coefficient	N/m	300000
Vertical sink speeds	m/s	2.1336 3.048

system consists of left and right side components, the flying car mass per landing gear is considered as the half of the flying car mass.

Bump passing manoeuvre is simulated using 2 different bump profiles: Parabolic and trapezoid. Bump height and bump length are set as 2 inches and 12 inches respectively for both bump profiles as shown on Figure 5 considering Uline brand standard bump profiles with model numbers H-6423 and H-4609 for parabolic and trapezoid bump profiles respectively [27].

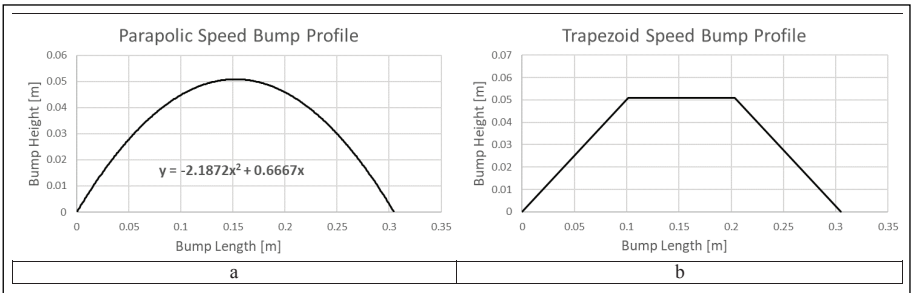

Figure 5. Parabolic Speed Bump Profile (a), Trapezoid Speed Bump Profile (b)

4. RESULTS

One landing and two bump passing manoeuvres with a duration of 4 seconds are simulated for the flying car using the vehicle and suspension system parameters listed in Table 2. Two different sink speed values are used in the landing manoeuvre: 7 and 10

ft/s (2.1336 and 3.048 m/s respectively) as per directions from Report: Decision No. 2003/14/RM of the Executive Director of The Agency [28]. Figure 6-a top plot shows the aircraft, shock absorber and suspension system displacements in black, blue and red colours respectively for the landing manoeuvre with 7 ft/s sink speed. Due to the weight (subtracting the lift) of the aircraft and the suspension system, there is 47.5 mm equilibrium displacement on the aircraft mass as shown with black colour. Tire maximum and equilibrium displacement values are simulated as 35.6 mm and 6.6 mm. The shock absorber equilibrium displacement is calculated as 40.9 mm. From the equilibrium position, shock absorber is compressed with a maximum value of 135.9 mm and extended with a maximum value of 50 mm, making the total travel of the shock absorber as 185.9 mm. Force applied to the aircraft mass during the landing manoeuvre is depicted in Figure 6-a central plot. The maximum force observed in during the landing manoeuvre is 10708 N. Aircraft acceleration values are depicted in Figure 6-a bottom plot and a maximum acceleration value of 14.28 m/s^2 is observed.

Figure 6-b top plot shows the aircraft, shock absorber and suspension system displacements in black, blue and red colours respectively for the landing manoeuvre with 10 ft/s sink speed. Equilibrium displacements are the same for both sink speed values. Maximum tire displacement is simulated as 4.9 mm. Total travel of the shock absorber is simulated as 272.9 mm with compression and extension values of 240.7 mm and 32.2 mm respectively. Force applied to the aircraft mass during the landing manoeuvre is depicted in Figure 6-b central plot. The maximum force observed in during the landing manoeuvre (with the same sink speed of the NACA experiment), is 15728 N. Aircraft acceleration values are depicted in Figure 6-b bottom plot and a maximum acceleration of 20.97 m/s^2 is observed.

Bump passing manoeuvres are simulated for 4 seconds with two longitudinal vehicle speed values: 5 kph and 10 kph. Parabolic bump passing manoeuvre results are shown at Figure 7-a and 7-b for 5 kph and 10 kph vehicle speeds respectively. Considering 5 kph bump passing manoeuvre; in the top plot of figure 7-a bump profile is shown with green colour and aircraft mass, shock absorber and suspension system displacements with respect to equilibrium position are shown with black, blue and red colours respectively. Maximum displacement of 48.6 mm is observed at the aircraft chassis resulting to a shock absorber maximum deformation (compression) of 29.7 mm. Maximum shock absorber extension is simulated as 39.7 mm summing the total travel of 69.4 mm. For this manoeuvre an absolute maximum value of 1772.2 N force applied to the chassis via the shock absorber and 4.73 m/s^2 acceleration is observed for compression direction. Considering extension direction 2886 N maximum force is observed at the shock vehicle chassis resulting to a maximum acceleration of 7.7 m/s^2.

Parabolic bump passing results manoeuvre with a vehicle longitudinal speed of 10 kph are shown at Figure 7-b. In the top plot bump profile is shown with green colour

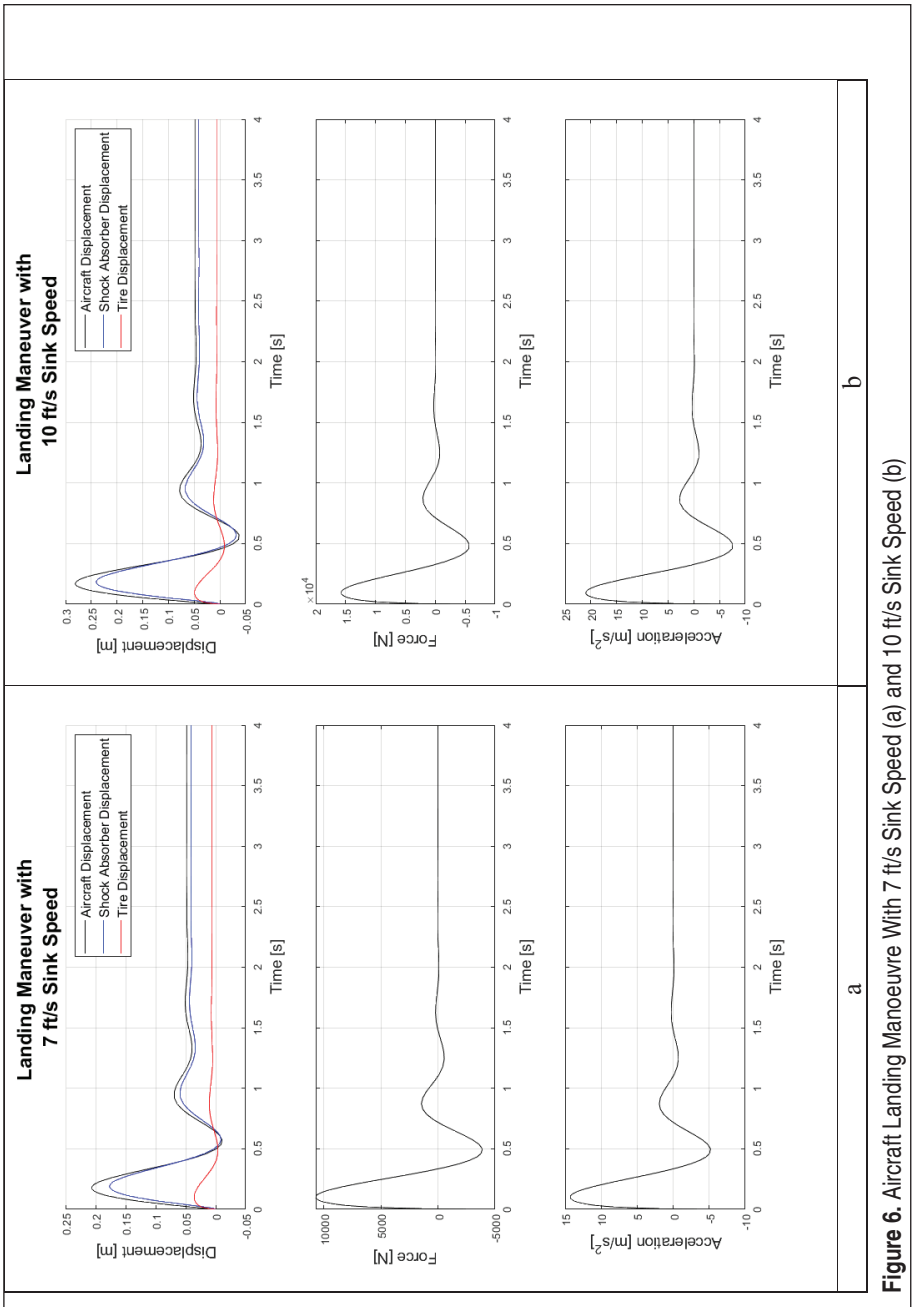

Figure 6. Aircraft Landing Manoeuvre With 7 ft/s Sink Speed (a) and 10 ft/s Sink Speed (b)

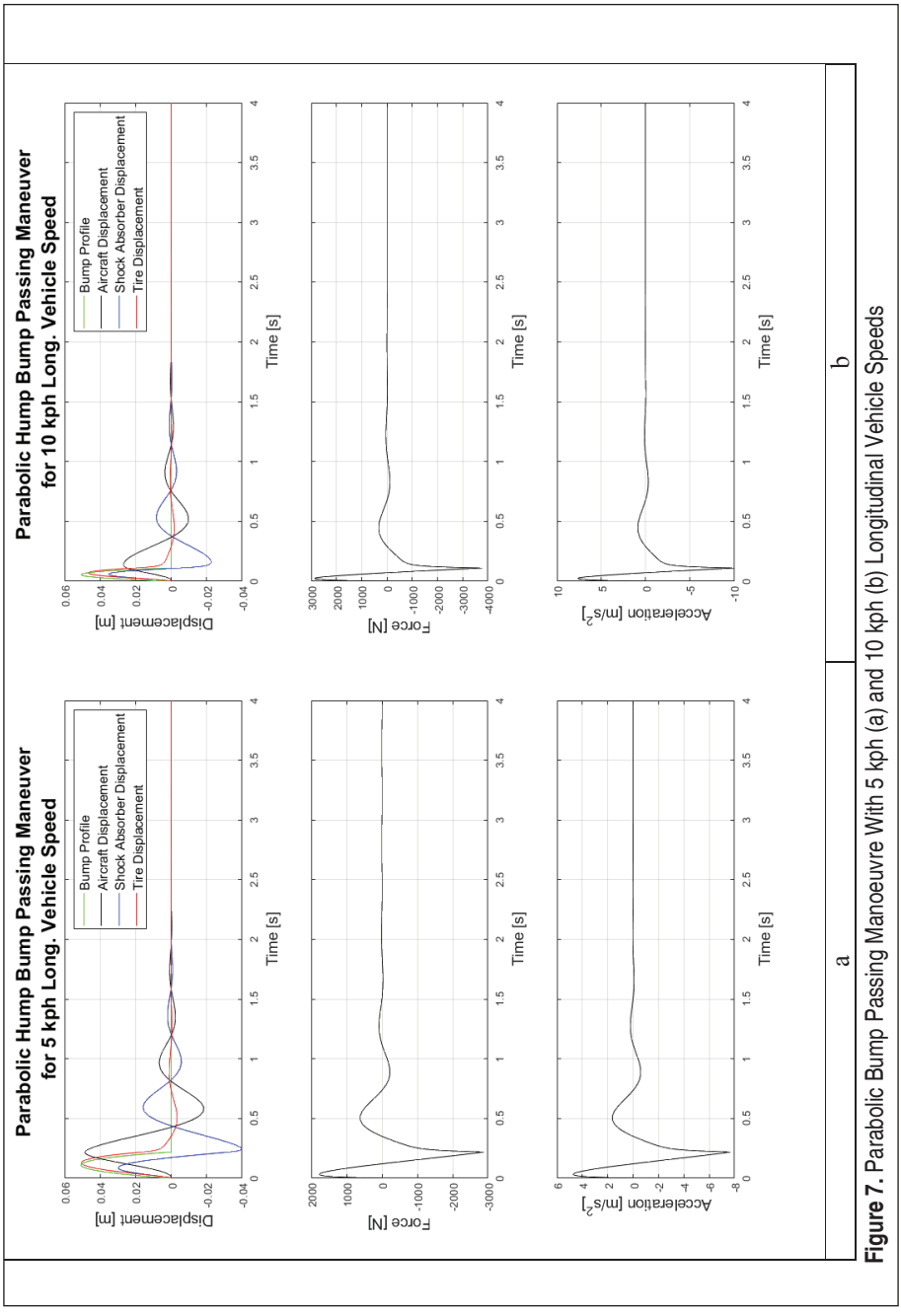

Figure 7. Parabolic Bump Passing Manoeuvre With 5 kph (a) and 10 kph (b) Longitudinal Vehicle Speeds

and aircraft mass, shock absorber and suspension system displacements are shown with black, blue and red colours respectively. Compared to 5 kph longitudinal vehicle speed a maximum displacement of 26.7 mm is observed at the aircraft chassis resulting to a shock absorber deformation of 35.3 mm in compression and 22.5 mm in extension directions. Shock absorber total travel is simulated as 57.8 mm. For this manoeuvre an absolute maximum of 7.65 m/s^2 acceleration is observed resulting to a force with maximum 2870 N for compression direction. For the extension direction 3774 N maximum force is observed at the shock vehicle chassis resulting to a maximum acceleration of 10.06 m/s^2.

Trapezoid bump passing manoeuvre for 5 kph longitudinal speed results are shown in Figure 8-a. Top figure shows bump profile, aircraft mass, shock absorber and suspension system displacements signals with green, black, blue and red colours respectively. A maximum value of 49.2 mm aircraft chassis displacement is observed. Maximum shock absorber deformations are simulated as 40.3 mm and 33.1 mm respectively for extension and compression directions summing the total travel of 73.4 mm. For this manoeuvre an absolute maximum value of 1923.5 N force applied to the chassis via the shock absorber and 5.13 m/s^2 acceleration is observed for compression direction. For the extension direction 2630 N maximum force is observed at the shock vehicle chassis resulting to a maximum acceleration of 7.01 m/s^2.

10 kph longitudinal vehicle speed trapezoid bump passing manoeuvre displacement results are shown in Figure 7-b for bump profile, aircraft mass, shock absorber and suspension system displacements signals with green, black, blue and red colours respectively. 26.9 mm maximum aircraft chassis movement is observed. Maximum shock absorber travels are simulated as 36.3 mm and 22.7 mm in compression and extension directions respectively, making the total travel as 59 mm. For the compression direction 3430 N maximum force is observed at the shock vehicle chassis resulting to a maximum acceleration of 9.15 m/s^2. For the extension direction 3533 N maximum force is observed at the shock vehicle chassis resulting to a maximum acceleration of 9.42 m/s^2.

Considering landing manoeuvres, setting time is defined as the duration that the aircraft position settles in %98 of the steady-state value. For the bump passing manoeuvres, setting time is defined as the duration that the vibrations are dampened within 2% of the bump height. Simulation results are summarized in Table 3. For the landing manoeuvre vibrations are dampened in around 1.9 seconds for both sink speeds. Considering bump passing manoeuvres is 1.5 and 1.37 seconds for the 5 kph and 10 kph longitudinal vehicle speed conditions. Shock absorber strokes are maximum for the landing manoeuvres due to the reason that when the aircraft is in the air just before landing, shock absorber goes to maximum extension length. Similarly maximum force is observed at the 10 ft/s landing manoeuvre.

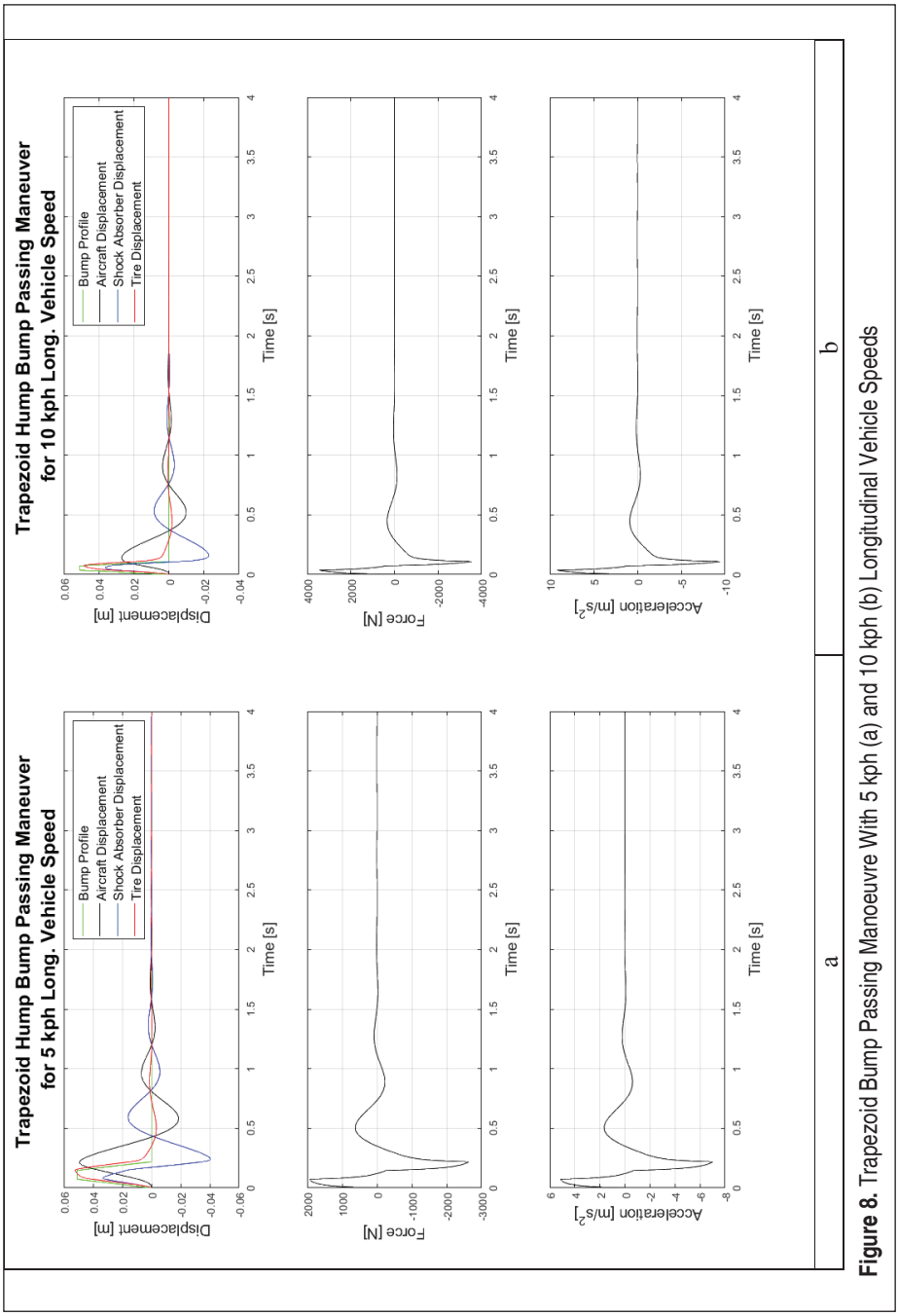

Figure 8. Trapezoid Bump Passing Manoeuvre With 5 kph (a) and 10 kph (b) Longitudinal Vehicle Speeds

Table 3. Matlab/Simulink Simulation Results

MANEUVER	Sink Speed (ft/s)	Long. Veh. Speed. (kph)	Comp. Dir. Max Force (N)	Comp. Dir. Max Accel (m/s^2)	Ext. Dir. Max Force (N)	Ext. Dir. Max Accel (m/s^2)	Set. Time (s)	Shock Absor. Stroke (mm)
LANDING	7	NA	10708	14.28	3935	5.25	1.87	177.4
LANDING	10	NA	15728	20.97	5742	7.66	1.88	272.9
B.P. – PARA.	0	5	1772	4.73	2886	7.7	1.5	69.4
B.P. – PARA.	0	10	2870	7.65	3774	10.06	1.37	57.8
B.P. – TRAP.	0	5	1924	5.13	2630	7.01	1.5	73.4
B.P. – TRAP.	0	10	3430	9.15	3533	9.42	1.38	59

5. DISCUSSION

Considering flying cars, suspension system should satisfy performance requirements for both landing and on road driving conditions. Within this perspective, it is proved out that the designed system with the suspension system parameters listed in Table 2, is adequate to meet the landing and bump passing requirements. For the landing manoeuvre the maximum achieved g-force is around 2.13 and the shock absorber stroke is around 273 mm which are within the expected range for small aircrafts. Moreover for the bump passing manoeuvres on road, considering the worst case scenario as 10 kph longitudinal vehicle speed, maximum accelerations are less than 1 g, considering the unsmoothed trapezoid bump profile, flying car will provide a comfortable ride. Choosing suspension system parameters as described in the study, will provide smooth landing and bump passing manoeuvres. Final tunning of the suspension system parameters should be performed depending on suspension system geometry.

6. CONCLUSION

Suspension system design is very critical for roadable aircrafts considering the fact that, the system should meet the criteria for both landing and on road maneuvers. Therefore suspension system parameters such as shock absorber spring and damping coefficients need to be optimized considering both maneuvers. In aviation industry optimization process is performed using simulations. Within this perspective a suspension system model is developed in Matlab/Simulink software that is able to simulate both landing and bump passing maneuvers. After validating the developed model using literature data for the landing maneuver, the model is employed to simulate landing and bump passing maneuvers for a roadable aircraft employing small size on road vehicle parameters. Results indicate that choosing suitable suspension system parameters will meet the criteria for both landing and bump passing maneuvers such as having a maximum acceleration value about 2.14 g with maximum shock absorber

displacement of 273 mm for the worst-case landing scenario with sink speed 10 ft/s. Considering the bump passing maneuvers, a maximum acceleration around 1 g is obtained in the extension direction for the 10 kph longitudinal vehicle speed for the parabolic bump profile.

REFERENCES

1. **Stiles, Palmer.** "CaRnard - A New Roadable Aircraft Concept." SAE Technical Paper Series, January 1993.
2. https://en.wikipedia.org/wiki/Roadable_aircraft#cite_ref-Time-never-come_7-0
3. **Kettering, Mark, and Daniel, Biezad.** "The Roadable Aircraft Design Project." 6th Symposium on Multidisciplinary Analysis and Optimization, April 1996.
4. **Follmann, Zsolt Eugenio Geza, and Adilson Marques Da Cunha.** "Triphibian Flying Car Design." SAE Technical Paper Series, January 1997.
5. **Crow, Steven.** "A Practical Flying Car." 1997 World Aviation Congress, 1997.
6. **Sarh, Branko, and Gunnar, Clausen.** "Private Air Transportation with Advanced Flying Automobiles and Roadable Aircraft and Impact on Intercity and Metropolitan Infrastructures." AIAA and SAE, 1998 World Aviation Conference, 1998. https://doi.org/10.2514/6.1998-5536.
7. Ott, Wolfgang. "HELIos, a VTOL Flying Car." SAE Technical Paper Series, 1998. https://doi.org/10.4271/985535.
8. **Nakajima, Madoka, Toichi Fukasawa, Hiroshige Kikukawa, and Atsushi Yanagisawa.** "Design of a Roadable Aircraft of Fixed Wing and the Investigation of the Aerodynamic Characteristics." SAE Technical Paper Series, February 2004. https://doi.org/10.4271/2004-01-3124.
9. **Nakajima, Madoka, Yutaka Nishimiya, and Hiroshige Kikukawa.** "Aerostructual Study on Inflatable Wing of a Roadable Aircraft." 48th AIAA/ASME/ASCE/AHS/ASC Structures, Structural Dynamics, and Materials Conference, 2007. https://doi.org/10.2514/6.2007-2330.
10. **Murai, M., and Hayashi, T.** (2006). A conceptual design of a Roadable aircraft. 25th International Congress of Aeronautical Sciences.
11. **Haskins, David, and David M. Haskins.** "The Pulsed Turbine Rotor Engine VTOL Propulsion Concept and Applications: Capturing the Elusive Jet-Powered Flying Car and Redesigning a Radical Variant of the V-22 Osprey." SAE Technical Paper Series, 2008. https://doi.org/10.4271/2008-01-2269.
12. **Saeed, B., and G. B. Gratton.** "An Evaluation of the Historical Issues Associated with Achieving Non-Helicopter V/STOL Capability and the Search for the Flying Car." The Aeronautical Journal 114, no. 1152 (2010): 91–102. https://doi.org/10.1017/s0001924000003560.
13. **Giannini, Francesco, Antoine Deux, Harold Youngren, and Robert Parks.** "Configuration Study and Performance of a Military V/STOL Roadable Aircraft." 11th AIAA Aviation Technology, Integration, and Operations (ATIO) Conference, 2011. https://doi.org/10.2514/6.2011-6997.

14. **Eker, Uğur, Grigorios Fountas, Panagiotis Ch. Anastasopoulos, Stephen E.** Still, An exploratory investigation of public perceptions towards key benefits and concerns from the future use of flying cars, Travel Behaviour and Society, Volume 19, 2020, Pages 54-66.
15. **Ahlin, Kjell, Granlund, Johan.** Calculation of Reference Ride Quality, using ISO 2631 Vibration Evaluation. 36th United Kingdom Group Meeting on Human Response to Vibration, UK, 2001
16. **Konieczny, Łukasz.** "Analysis of Simplifications Applied in Vibration Damping Modelling for a Passive Car Shock Absorber." Shock and Vibration 2016 (2016): 1–9. https://doi.org/10.1155/2016/6182847.
17. **Darsivan, Fadly Jashi, and Waleed F. Faris.** "Vibration Investigation of a Quarter Car with Nonlinear Shock Absorber Model." Advanced Materials Research, vol. 576, 2012, pp. 665–668., doi:10.4028/www.scientific.net/amr.576.665.
18. **Luczko, Jan, and Urszula Ferdek.** "Non-Linear Analysis of a Quarter-Car Model with Stroke-Dependent Twin-Tube Shock Absorber." Mechanical Systems and Signal Processing 115 (2019): 450–68. https://doi.org/10.1016/j.ymssp.2018.06.008.
19. **Jahromi, Ali Fellah, and A. Zabihollah.** "Semi Active Vibration Control of a Passenger Car Using Magnetorheological Shock Absorber." ASME 2010 10th Biennial Conference on Engineering Systems Design and Analysis, Volume 3, Jan. 2010, doi:10.1115/esda2010-24079.
20. **Devdutt, and M. L. Aggarwal.** "Fuzzy Control of Passenger Ride Performance Using MR Shock Absorber Suspension in Quarter Car Model." International Journal of Dynamics and Control, vol. 3, no. 4, 2014, pp. 463–469., doi:10.1007/s40435-014-0128-z.
21. W. Flugge, Landing Gear Impact, NACA, TN2743, 1952
22. **B. Milwitzky, F.E.** Cook, "Analysis of Landing-Gear Behavior", NACA, TN1154, 1953
23. H.G. Conway, Landing Gear Design. Chapman & Hall, 1958
24. N.S. Currey, Aircraft Landing Gear Design Principles and Practices Aiaa Education Series,1988
25. **Karam, W, and J-C Mare.** "Advanced Model Development and Validation of Landing Gear Shock Struts." Proceedings of the Institution of Mechanical Engineers, Part G: Journal of Aerospace Engineering 224, no. 5 (February 2009): 575–86. https://doi.org/10.1243/09544100jaero602.
26. **Pratomo, Wanda, M. Adhitya, and Putra Mulya P.** "Design and Analysis of Upper Wishbone for Suspension System on Vertical Take-off and Landing (VTOL) Propulsion System Flying Car," AIP Conference Proceedings 2008. https://doi.org/10.1063/1.5051978.
27. Uline Catalog, "Uline." https://catalog.uline.com/Spring-Summer-US-2022/720/ [Retrieved: 29-March-2022]
28. ED Decision 2003/14/RM, "EASA.", https://www.easa.europa.eu/sites/default/files/dfu/decision_ED_2003_14_RM.pdf [Retrieved: 29-March-2022]